Research Square

Preprints are preliminary reports that have not undergone peer review.
They should not be considered conclusive, used to inform clinical practice,
or referenced by the media as validated information.

Smart Geospatial Analytics for Climate-Resilient and Sustainable Futures: Urban Heat Islands and Hotspots Mapping in Greater Francistown City, Botswana

Bongayi Kudoma

makovabong@gmail.com

University of Witwatersrand

Research Article

Keywords: Urban Heat Island, Climate Change, Remote Sensing, Land Surface Temperature, Smart Solution, Geospatial Analysis, Climate Resilience, Sustainable Futures

Posted Date: November 10th, 2026

DOI: https://doi.org/10.21203/rs.3.rs-11272684/v1

License: This work is licensed under a Creative Commons Attribution 4.0 International License.
Read Full License

Additional Declarations: No competing interests reported.

Smart Geospatial Analytics for Climate-Resilient and Sustainable Futures: Urban Heat Islands and Hotspots Mapping in Greater Francistown City, Botswana.

Bongayi Kudoma[1,2] ORCID- 0000-0001-9920-5417

[1] University of Witwatersrand, School of Geography, Archaeology and Environmental Studies, Johannesburg, South Africa.

[2] BA ISAGO University, Department of Safety Management, Francistown, Botswana.

bongayi.kudoma@baisago.ac.bw, Francistown, Botswana, makovabong@gmail.com, +267 73235979

Abstract

Urban Heat Islands (UHI) are critical indicators of urban climate change in rapidly urbanising regions of the Global South. This study applied smart geospatial analytics and remote sensing-based climate information systems to analyse the spatial distribution, intensity, temporal dynamics of the UHI and urban hotspot effects in Greater Francistown City between 2014 and 2023. Using Landsat 8 Operational Land Imager and Thermal Infrared Sensor data, Land Surface Temperature was derived to support climate monitoring, resilient infrastructure planning, and climate-responsive urban design. Results reveal notable spatiotemporal variability in urban thermal patterns, with UHI intensity showing fluctuations from 6.05 km² in 2016 to 4.71 km² in 2019, concentrated in densely built-up areas. Urban hotspot precincts increased from 1.59 km² in 2016 to 2.44 km² in 2023, reflecting land-use transformation and vegetation loss. These findings highlight the role of digital environmental monitoring tools and smart city approaches in identifying climate risk zones and supporting evidence-based urban planning. The study demonstrates how geospatial data analytics and Earth observation technologies enhance climate information systems, providing actionable insights for sustainable urban development. It underscores the integration of smart, data-driven approaches into planning frameworks to mitigate heat stress, improve environmental quality, and strengthen climate resilience in semi-arid cities. Positioning Greater Francistown as a Global South case study, the findings advance digital solutions for climate modelling and monitoring, contributing to the Sustainable Development Goals and climate-resilient, smart, and sustainable futures.

Policy action is recommended to embed UHI mitigation into zoning regulations, building standards, and incentives for heat-resilient infrastructure.

Keywords
Urban Heat Island, Climate Change, Remote Sensing, Land Surface Temperature, Smart Solution, Geospatial Analysis, Climate Resilience, Sustainable Futures

1. Introduction

Climate change and global warming have intensified heat stress in urban environments, driving significant increases in land surface temperatures (LST) [44, 18, 26]. Rising urban temperatures [64] lead to thermal accumulation, making cities consistently warmer than surrounding rural areas [42,6,68]. This phenomenon, known as the Urban Heat Island (UHI) effect [14,82], is a direct consequence of rapid urbanisation [28]. UHI mitigation requires strategies such as smart city planning, resilient infrastructure and green infrastructure solutions [80,13]. In the era of digital transformation, remote sensing and geospatial analytics have become essential for monitoring dynamics and supporting climate-responsive urban design [13]. Embedding these approaches into urban governance is critical for advancing the Sustainable Development Goals (SDGs), including Industry, Innovation, and Infrastructure (SDG 9), Sustainable Cities and Communities (SDG 11), and Climate Action (SDG 13). Moreover, in the Global South, inclusive resilience strategies are vital to ensure that adaptation measures address the vulnerabilities of rapidly urbanising populations [76, 2].

Urbanisation has reshaped cities into complex, dynamic systems that profoundly influence local climates and human well-being. The expansion of impervious surfaces, reduction of vegetation, and increased anthropogenic heat emissions intensify urban temperatures [31,43]. Addressing these impacts requires climate-responsive urban design, smart-city strategies, and resilient infrastructure that integrate geospatial monitoring and digital climate solutions [46,62]. 80 and 13 emphasise that green infrastructure and nature-based solutions are effective in mitigating UHI effects while enhancing urban sustainability. Embedding these innovations into planning frameworks not only reduces vulnerability to heat stress but also advances Sustainable Cities and Communities through inclusive and resilient urban development; Climate Action by strengthening adaptation to climate extremes; and

Industry, Innovation, and Infrastructure by leveraging digital technologies for sustainable growth [1,5,39]. Importantly, in the Global South, such approaches contribute to a just and inclusive climate resilience agenda, ensuring that adaptation strategies address the needs of vulnerable communities [1, 51, 75, 76].

Advances in remote sensing and geospatial analytics now enable high-resolution monitoring of thermal patterns [22], offering actionable insights for smart climate information systems that support resilient and sustainable urban planning. Remote sensing applications in UHI research have advanced considerably [24], enabling systematic analysis of surface urban heat islands (SUHI) across diverse cities [55, 33]. Landsat 8 imagery, in particular, has proven effective for evaluating UHI dynamics in rapidly urbanising regions [69]. [16] demonstrates the value of integrating Earth observation with smart geospatial platforms to strengthen climate resilience and inclusive urban planning in Global South contexts. These digital tools underscore the growing importance of Earth observation technologies in mapping spatiotemporal heat variability and informing sustainable urban design.

Evidence shows that UHI intensity is rising globally, with increases of 2.01 °C to 2.4 °C in major cities [60]. Botswana's urban centres are no exception and are projected to face some of Africa's highest temperature increases [7, 53]. Regional climate assessments confirm that southern Africa is warming at rates above the global average [20,67, 19], intensifying risks for semi-arid cities such as Francistown. This trend underscores the urgent need for digital climate monitoring systems and smart adaptation strategies to accelerate Botswana's efforts to build climate resilience. Integrating geospatial analytics with inclusive urban planning frameworks is increasingly recognised as essential for achieving equitable climate-resilient futures in the Global South [77, 8, 50, 51, 71]**.**

Despite extensive modelling of heat waves in cities, the UHI problem remains complex and persistent. Global warming and rapid urbanisation are expected to intensify UHI effects in the coming years. Francistown, Botswana's second city, is undergoing rapid urban growth, making it a critical case for assessing UHI intensity and exploring digital climate-monitoring solutions to inform sustainable urban planning. Population growth, urbanisation, and semi-arid climatic conditions have reshaped Francistown's microclimate, altering ecosystem functions and structures [53, 11,12]. The UHI effect

is increasingly pronounced, with built-up areas experiencing elevated temperatures during spring and summer [77]. These changes intensify heat stress for residents, underscoring the need for smart geospatial analytics and climate information systems to guide adaptive urban design [8, 71, 51]. Semi-arid urban centres in southern Africa are particularly vulnerable to intensifying heat stress, requiring smart geospatial analytics and climate information systems to guide adaptive urban design [20,19].

Francistown's temperatures are projected to surpass the 41.4 °C record set in 2011 [10, 47], with warming trends exceeding global averages [49]**.** Such extremes threaten the Paris Agreement's targets to limit warming below 2°C and highlight the urgency of deploying digital climate modelling and smart monitoring systems to anticipate risks and strengthen resilience [7]. Projections for southern Africa confirm that semi-arid regions are likely to experience more frequent and intense heat extremes, compounding risks for rapidly urbanising cities [19,48]. Despite rising concerns, Francistown lacks comprehensive research on the spatiotemporal dynamics of UHIs at the microclimate scale. Current development projections overlook UHI impacts, leaving critical knowledge gaps. Existing studies focus on heat waves [45, 70] and UHI in Gaborone [30, 53], underscoring the need for localised, data-driven climate assessments in Francistown.

These knowledge gaps highlight the need to quantify and map Francistown's UHI and urban hotspot dynamics between 2014 and 2023. Understanding spatiotemporal thermal patterns is essential for designing climate-resilient urban futures. This study is therefore motivated by the urgent need for microclimate-scale monitoring, using geospatial and remote sensing technologies, to provide evidence-based insights to guide sustainable urban development in semi-arid cities. Studies underscore that localised UHI assessments are critical for Global South cities, where rapid urbanisation and limited adaptive capacity heighten vulnerability [17, 77, 8, 51]. By situating Francistown as a case study, this study contributes to bridging regional knowledge gaps and advancing inclusive climate resilience strategies

To address these gaps, this study employs remote sensing and geospatial analytics to quantify Francistown's UHI dynamics from 2014 to 2023. The methodological framework focuses on Landsat 8 imagery and spatial analysis, providing evidence-based insights to guide sustainable urban planning in semi-arid contexts.

2 Material and Methods

2.1 Study Area Description

Francistown, Botswana's second-largest city (21°10′S, 27°30′E) (Fig 1), had a population of approximately 103,417 in 2022, covers 79 km², and is characterised by rapid urbanisation, semi-arid climatic conditions, and evolving land-use patterns that may influence its urban microclimate and heat stress [56; 53; 11]. The city experiences moderate to irregular rainfall [23], with an average annual total of approximately 460 mm, and temperatures ranging from –6.5 °C to 41.1°C and is susceptible to drought conditions associated with broader climatic variability in Botswana [9, 12; 40]. Although regional studies link urban land-use change in Botswana to increased land-surface temperatures and vegetation loss [25], direct longitudinal evidence quantifying Francistown's built-up expansion and localised UHI intensity remains limited. Nevertheless, the city provides a useful case for integrating remote sensing, geospatial monitoring, and climate data to assess ecological vulnerability and heat-stress patterns and to support sustainable urban planning [38].

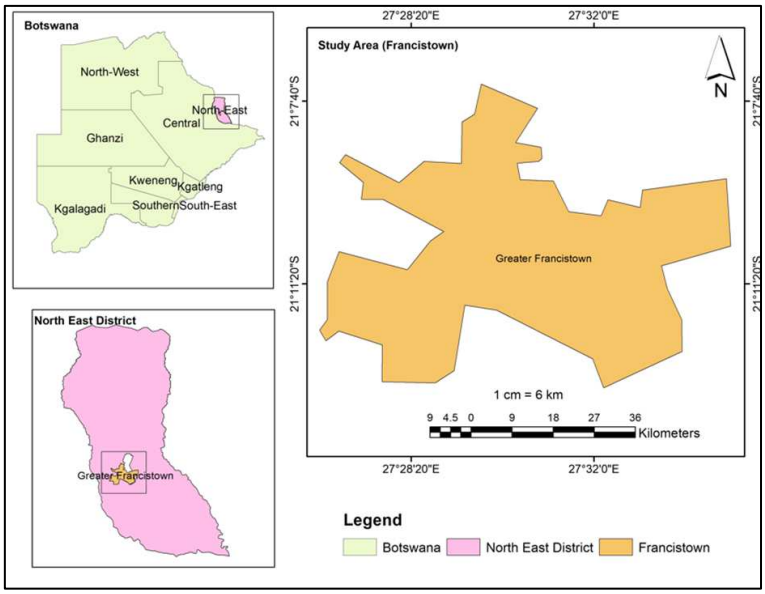


Fig 1 Location of Study Area

2.2 Research Design

This study employed an experimental research design to assess the spatiotemporal variability of UHI and urban hotspots in Greater Francistown City. Following the methodology outlined in the data acquisition section, the design sought to uncover

causal relationships between land use/land cover (LULC), land surface temperature (LST), and UHI intensity through controlled spatial analysis [65].

The workflow was structured into distinct tasks:

- Retrieval of LST and Normalised Difference Vegetation Index (NDVI) to classify UHI and non-UHI areas.
- Integration of GIS tools (QGIS, ArcMap) with statistical techniques (SAS) for spatial-temporal quantification.
- Application of Google Earth Engine (GEE), a cloud-based computing platform, to process Landsat datasets and enhance reproducibility [3, 81].

This design highlights the role of digital geospatial technologies and climate information systems in monitoring urban thermal dynamics. By combining Earth observation data with smart analytics, the study provides a replicable framework for evidence-based urban planning and climate resilience. It also ensures methodological transparency, enabling future comparative studies across semi-arid cities in southern Africa.

2.3 Data Acquisition

This study utilised Landsat 8 Operational Land Imager (OLI) and Thermal Infrared Sensor (TIRS-1) data to analyse UHI variability in Greater Francistown City between 2014 and 2023. Five time points (2014, 2016, 2019, 2021, 2023) were selected to capture the urban thermal change baseline, lower quartile, midpoint, upper quartile, and endpoint (2014-2023). Cloud-free Landsat OLI/TIRS imagery was sourced from the USGS Earth Explorer http://earthexplorer.usgs.gov/) and processed via the Google Earth Engine (GEE) catalogue, ensuring reproducibility and efficiency.

Landsat 8 provides spectral bands with 15–30 m resolution, which can be downscaled to 10 m when fused with Sentinel-2 [52]. The thermal infrared bands (10 and 11) provide 100 m resolution, enabling precise LST retrieval. The 11 spectral bands vary in wavelength from 0.433 μm to 12.51 μm (Table 1). The dataset's accessibility and proven reliability for UHI studies [72, 4, 78; 27, 32, 79, 57] make it ideal for long-term monitoring.

Image selection prioritised high-quality, low-cloud scenes across the study period, with a 16-day revisit cycle from 01 January 2014 to 31 December 2023**.** This digital workflow highlights the role of remote sensing and smart geospatial platforms in generating actionable climate data for sustainable urban planning.

Table 1 Description of the Landsat 8 dataset utilised in the study area

Sensor	**Description**	**Band**	**Spectral Range (micrometres)**	**Resolution**
Landsat 8 Tier-1	LST	10 TIRS-1	10.60 - 11.190	30/100 m
Landsat 8 OLI	NDVI	4-Red 5 Near-Infrared	0.640 - 0.670 0.850 - 0.880	30m 30m

Source [27]

2.4 Pre-Processing

Pre-processing was conducted to correct atmospheric, geometric, and radiometric errors in Landsat imagery, using the Google Earth Engine (GEE) platform for efficiency and reproducibility. Landsat 8 OLI and TIRS-1 datasets were filtered for the Greater Francistown City region, with cloud, aerosol, and shadow masking applied to ensure data quality [35]. Water pixels were excluded to avoid bias from high specific heat capacity, and final images were clipped to the city's shapefile boundaries. This streamlined digital workflow ensured accurate LST retrieval and reliable spatial analysis for UHI mapping.

2.4.1 Land Surface Temperature Calculations

Land Surface Temperature (LST) was derived from Landsat 8 OLI thermal band 10 (10.60–11.19 µm). Radiometric correction converted digital numbers (DN) to top-of-atmosphere (TOA) spectral radiance using Equation 1:

$$L_\lambda = M_L \text{ x } Q\text{Cal} + A_L \qquad \text{Equations [1]}$$

Where L_λ is TOA spectral radiance, M_L the band-specific multiplicative rescaling factor, $Q\text{Cal}$ the quantised and standardised product pixel value (DN), $\text{and } A_L$ the additive rescaling factor. This measurement is expressed in watts per square meter per steradian per nanometer (W/(m²·sr·nm)).

TOA Tie1 data from Landsat 8 were processed for 2014, 2016, 2019, 2021, and 2023, with median values calculated and clipped to the Greater Francistown City shapefile.

Spectral radiance L_λ was then converted to brightness temperature (TB) using Equation 2, assuming unit emissivity in Kelvin.

$$T_B = \frac{K_2}{\ln\left(\frac{K_1}{L_\lambda}+1\right)} \quad \text{Equations [2]}$$

Band-specific Thermal conversion constants were applied: K1 = 774.89 mW/cm²/sr/μm and K2 = 1321.08 K, ensuring accurate retrieval of thermal gradients. To improve LST retrieval accuracy, surface emissivity was estimated using NDVI-based threshold methods, which account for surface heterogeneity by assigning specific emissivity values to distinct built-up and vegetated land-cover classes [63, 29, 21]. This digital workflow highlights the role of remote sensing and smart geospatial analytics in producing reliable LST estimates for UHI mapping and climate resilience studies.

2.4.2 Land Surface Temperature Retrieval

The LST was retrieved from Landsat 8 imagery satellite for 10 years (2014 to 2023) using thermal infrared data and atmospheric correction algorithms. The Landsat 8 TIRS-1 band 10 (10.60-11.19 μm) with 30m resolution was utilised. The TIRS-1 is exceptionally sensitive to urban temperature variations due to its shorter wavelength and its ability to detect temperature gradients in urban areas, where UHI effects are very noticeable [26].

Land surface temperature was retrieved from Landsat 8 TIRS-1 band 10 (10.60–11.19 μm, 30 m resolution) for the period 2014-2023, applying atmospheric correction algorithms to ensure accuracy. Band 10 is highly sensitive to urban temperature variations, making it suitable for detecting UHI-related temperature gradients [26].

Landsat 8's spatial and temporal coverage provides reliable datasets for LST estimation, valued for its precision and accessibility [15, 74.] Conversion from satellite brightness temperature to LST in Celsius was performed using Equation 3, incorporating physical constants (Planck's constant, Boltzmann constant, and speed of light). Radiant temperatures were corrected by subtracting absolute zero (–273.15 °C).

$$\mathrm{LST}(^{o}\mathrm{C}) = \frac{T_B}{\left[1+\left(\lambda\times\frac{T_B}{\rho}\right)\ln(e)\right]} - 273.15 \quad \text{Equations [3]}$$

Where λ is the wavelength of the radiated radiance, = h(c/s) = 1.4388 102m K = 14388 m K, h is Planck's constant = 6.626 1034Js, s is the Boltzmann constant = 1.38 1023J/K, and c is the velocity of light = 2.998 108m/s. This digital workflow demonstrates how remote sensing and smart geospatial analytics enable consistent monitoring of urban thermal dynamics, providing actionable data for climate-resilient urban planning.

2.5 Calculations of Spatiotemporal Parameters of UHI

2.5.1 Mapping of the UHI and Non-UHI

The UHI distribution and development vary across cities, influenced by factors such as LST [55]. UHI distribution and intensity were quantified by comparing urban and non-urban LST values using Equations 4 and 5.

$$\mathrm{UHI} = \mathrm{LST} > \mu + 0.5 * \delta \quad \text{Equation [4]}$$

$$\text{Non- UHI } = 0 < \mathrm{LST} \leq \mu + 0.5 * \delta \quad \text{Equations [5]}$$

Mean (μ) and standard deviation (δ) of LST were applied to classify elevated temperature zones. To improve accuracy, land use/land cover (LULC) maps were integrated with LST outputs, thereby ensuring precise delineation of heat island regions and reducing misclassification in transitional zones.

2.5.2 Mapping Urban Hot Spot Areas

The Urban Hot Spots (UHS) areas for Greater Francistown City were computed using Equation 6, which represents spatial clusters of high LST within built-up areas [58].

$$\mathrm{UHS} = \mathrm{LST} > \mu + 2 * \sigma \quad \text{Equations [6]}$$

Thresholds were determined using statistical percentiles of LST values to ensure consistency across the five study years (2014, 2016, 2019, 2021, 2023). This combined approach linking statistical thresholds with geospatial mapping highlights the role of digital remote sensing and smart analytics in detecting climate risk zones and supporting sustainable urban design.

3 Results

3.1 Spatiotemporal Distribution of UHI and non-UHI

Fig. 2 depicts the UHI and non–UHI status in Greater Francistown City at the five time points of 2014, 2016, 2019, 2021, and 2023.

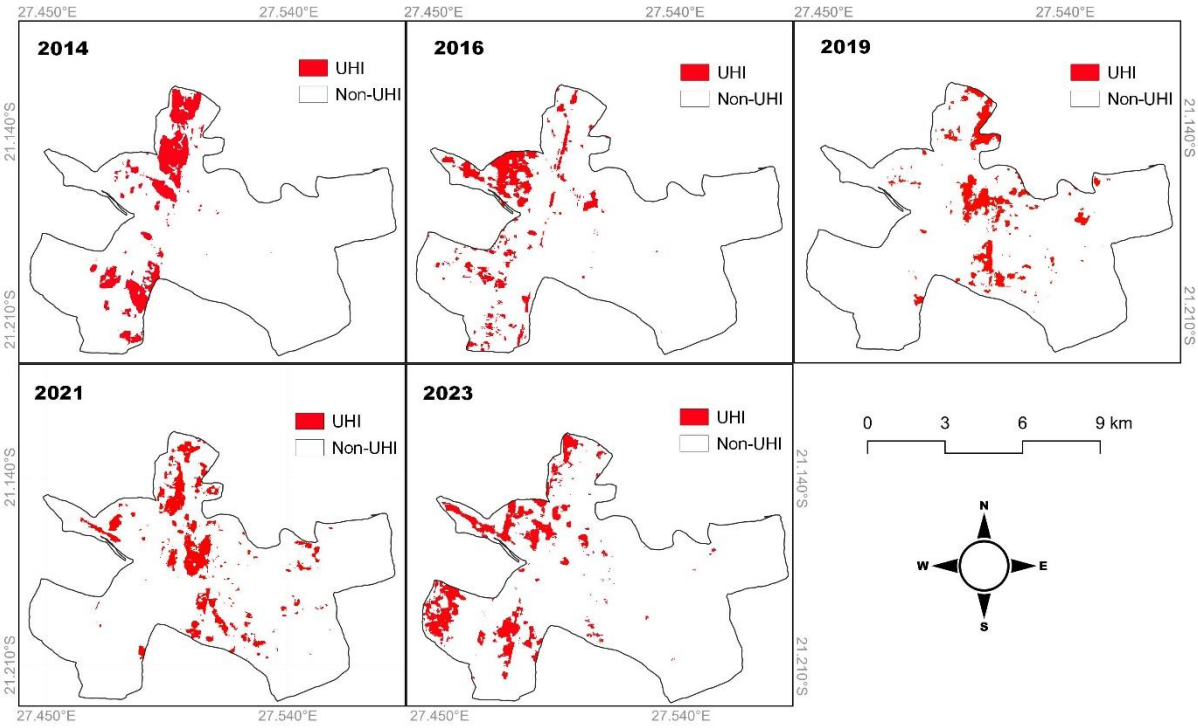


Fig 2 Greater Francistown City Identified UHI and Non-UHI

Table 2 summarises areas and the percentages of Greater Francistown City's UHI, non-UHI, and Urban hotspot precincts. The UHI was mainly observed in the city's built-up and bare land precincts. These areas grew from the Southwest to the Northwest from 2014 to 2016, expanded from the city's centre to the northern area in 2019-2021, and extended to the southwest in 2023, following the spatial patterns of LULC and LST changes.

Table 2 . Spatiotemporal Variations of UHI, non-UHI, and Urban Hotspot Areas

	2014		2016		2019		2021		2023	
Class	**Area km²**	**%**	**Area km²**	**%**	**Area km²**	**%**	**Area km²**	**%**	**Area km²**	**%**
UHI	6.05	7.74	5.19	6.64	4.71	6.03	5.84	7.48	6.62	8.47
Non-UHI	72.07	92.26	72.93	93.36	73.41	93.97	72.28	92.54	71.49	91.53

UHS	3.02	3.87	1.59	2.04	1.88	2.41	2.02	2.59	2.44	3.12

In 2014, 6.05 km² (7.74%) of the Greater Francistown city was classified as UHI, largely concentrated in bare-land precincts. The UHI extent declined to 4.71 km² (6.03%) in 2019, before rising again to 6.62 km² (8.47%) in 2023, reflecting the city's rapid expansion and land-use change. The period from 2021 (7.45%) to 2023 (8.47%) saw a 0.99% increase in the total area classified as UHI (Table 2). The average LST values for UHI were estimated at 35.13 °C (2014), 37.80 °C (2016), 39.61 °C (2019), 36.89 °C (2021), and 35.43 °C (2023). This range (35–40 °C) confirms the strong link between impervious surfaces, vegetation loss, and heat retention.

These results demonstrate the strong correlation between urban growth patterns and UHI intensity. The occurrence of UHI in the city can raise climatic and environmental concerns, potentially affecting individuals' general welfare. Furthermore, 2023 confirms the growth of UHI regions. This underscores the need for digital climate monitoring systems to track spatiotemporal variability and guide adaptive planning. By integrating geospatial analytics into climate information systems, cities like Francistown can identify risk zones and design resilience strategies that mitigate heat stress.

Conversely, the non–UHI areas were extensive in the Northern and Southern regions of the city, covering 72.07 km^2 (92.26%) in 2014, 72.28% in 2019, and 91.53% in 2023, as indicated by the white colour in Fig 3. The non–UHI area decreases across the study area as the UHI area increases.

3.2 Spatiotemporal Distribution of Urban Hotspots

Fig 3 depicts the Urban Hotspot (UHS) in Greater Francistown City at five time points: 2014, 2016, 2019, 2021, and 2023, based on the LST analysis. The identified UHS were distributed in a few extremely concentrated areas in the bare land and built-up areas.

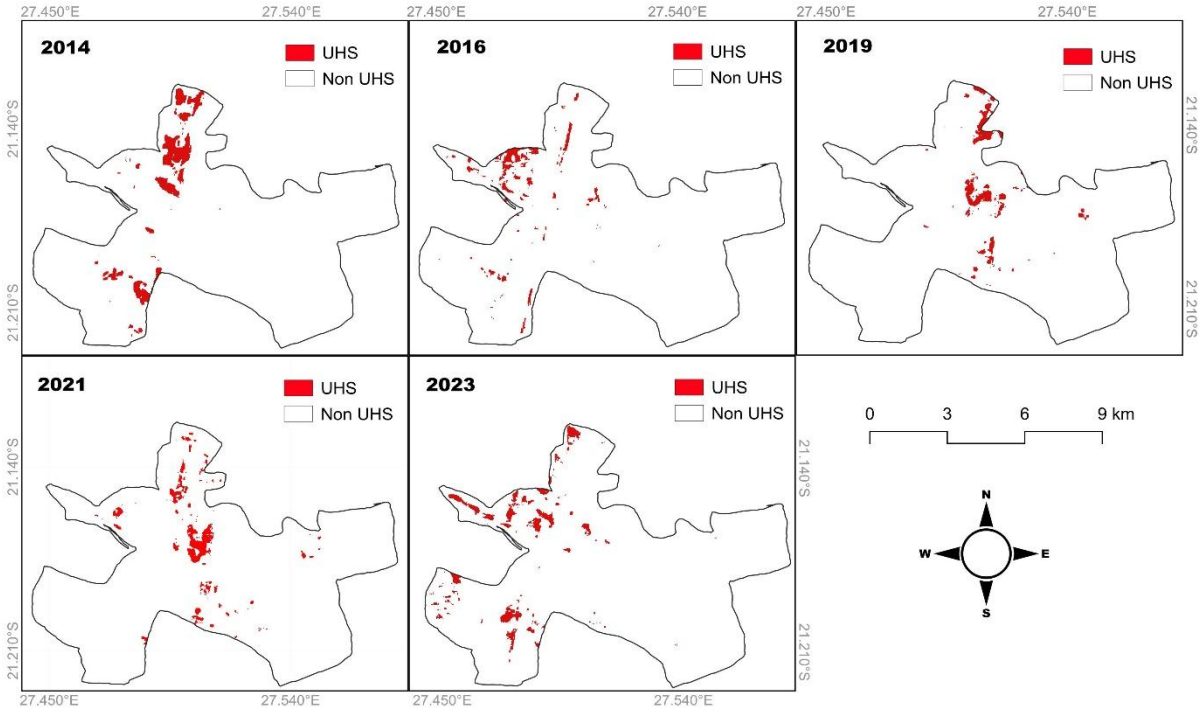


Fig 3 Greater Francistown City Identified Urban Hotspot

Urban Hotspot precincts declined from 3.02 km² (3.87%) in 2014 to 1.59 km² (2.04%) in 2016, then expanded to 2.44 km² (3.12%) in 2023 (Fig 3), representing a 1.08% increase in UHS. The UHS exhibits less significance in water bodies and vegetation areas. In 2014, the UHS area was 3.02 km^2 (3.87%).

These hotspots were concentrated on bare land, in industrial zones, on metal roofs, and in parking bays, while vegetation and water bodies showed minimal heat accumulation. By 2023, 75.68 km^2 (96.88%) of the city remained free of hotspots, indicating localised but intensifying thermal stress. These thresholds provide a quantitative benchmark for identifying risk zones and prioritising interventions.

The identification of UHS thresholds were 40.02°C, 43.27°C, 40.86°C, 37.47°C, 40.06°C, 42.45°C, 40.27°C, 40.07°C, 40.07°C and 38.10°C for 2014-2023 (ranging from 37.47 °C to 43.27 °C) highlights the precision of remote sensing and geospatial analytics in detecting microclimate extremes. Embedding these insights into smart climate information systems enables proactive resilience planning by targeting vulnerable precincts with cooling interventions, such as green, reflective, and permeable surfaces.

4 Discussions

The results confirm that UHI intensity in Francistown is strongly associated with bare land and built-up precincts, where impervious surfaces and reduced vegetation amplify heat retention. The fluctuations observed between 2014 and 2023 reflect the dynamic interplay of land-use change, urban expansion, and climatic variability [66, 59, 36]. The resurgence of UHI extent after 2021 underscores the need for continuous high-resolution digital monitoring to anticipate thermal risks and guide adaptive interventions. Recent work on smart city digital twins demonstrates how integrated climate data can be used to forecast collective urban heat exposure and support proactive resilience planning [54].

The environmental implications are significant: elevated LST values increase energy demand, degrade air and water quality, and intensify health risks during heat waves [37, 34, 41]. These findings highlight the urgency of embedding smart climate information systems into urban governance to enable early warning, targeted cooling strategies, and resilience planning. Advances in big-data-driven prediction models now enable intelligent forecasting of UHI dynamics, strengthening the evidence base for sustainable urban design [73].

Conversely, the persistence of non-UHI zones in vegetated and open areas demonstrates the cooling potential of green infrastructure and ecosystem-based solutions. This reinforces the importance of integrating nature-based approaches with digital geospatial analytics to design sustainable urban futures. A recent global study using open data and collaborative technology confirms that combining vegetation mapping with UHI monitoring enhances resilience in rapidly urbanising regions [61].

Urban Hotspot analysis further revealed localised but intensifying heat stress, concentrated in industrial zones, metal-roofed structures, and parking bays. The identification of UHS thresholds (37-43 °C) illustrates the precision of remote sensing and geospatial technologies in detecting microclimate extremes. Embedding these insights into smart urban planning frameworks can support targeted interventions such as reflective surfaces, shading, and urban greening.

Overall, the study demonstrates how digital transformation in climate monitoring, enabled by remote sensing, geospatial analytics, and smart information systems, provides actionable evidence for sustainable urban design. By linking thermal

dynamics to resilience strategies, Francistown offers a model for semi-arid cities seeking to balance rapid urbanisation with climate-smart sustainability.

5 Conclusion

This study demonstrates that the spatial patterns of Urban Heat Island intensity and thermal hotspot dynamics in Francistown are closely associated with rapid urbanisation, land-use change, and vegetation loss. By integrating geospatial analytics and Earth observation technologies, the study generates spatially explicit evidence that can inform climate information systems and support more sustainable urban development. The findings highlight the value of integrating smart, data-driven approaches into urban planning frameworks to identify heat-vulnerable areas, guide targeted intervention, reduce heat stress, improve environmental quality, and strengthen resilience in semi-arid cities.

As a global South case study, Francistown city illustrates the challenges and opportunities associated with managing urban heat in rapidly urbanising contexts. The study contributes to a more just and inclusive climate-resilience agenda by demonstrating how locally grounded geospatial evidence can support climate-responsive planning and governance. Its findings align with SDG 11 (Sustainable Cities and Communities) by supporting more resilient and sustainable urban development, SDG 13 (Climate Action) by informing climate-risk monitoring and adaptation, and SDG 9 (Industry, Innovation, and Infrastructure) through the application of digital technologies for climate modelling, environmental monitoring, and decision support. More broadly, the study offers transferable insights into how smart, climate-resilient, and context-sensitive planning approaches can contribute to sustainable urban futures.

6 Policy Recommendations

To effectively mitigate UHI impacts in Greater Francistown City, government authorities should adopt and enforce a comprehensive urban heat resilience policy that integrates zoning regulations for green spaces, mandates the use of cool roofs and energy-efficient building materials, and incentivises developers to implement sustainable, heat-resilient practices. Establishing clear standards and guidelines for climate-responsive infrastructure will ensure that all new developments account for

thermal risks, thereby safeguarding public health, enhancing environmental quality, and strengthening long-term urban resilience.

7 Limitations and Future Research Directions

This study offers valuable insights into UHI dynamics in Greater Francistown City but has several limitations. Reliance on Landsat 8 imagery, with moderate resolution and a 16-day revisit cycle, may miss finer temporal variations. Limited ground-based climate and health data constrained validation and direct linkage to human exposure, while focusing on a single semi-arid city, restricts wider generalisability.

Future research should employ higher-resolution datasets (Sentinel-2, MODIS, UAV imagery), expand ground-truthing using local climate stations, and apply machine-learning models for predictive UHI mapping. Comparative studies across southern African cities and integration of socio-economic vulnerability assessments would strengthen regional relevance. Policy-oriented research is also needed to evaluate zoning regulations, green infrastructure incentives, and heat-resilient building standards, ensuring scientific evidence informs urban governance and climate adaptation.

Acknowledgements

I gratefully acknowledge the University of the Witwatersrand for academic support during my MSc in GIS and Remote Sensing, and the organisers of ICCRSSF 2026 for providing a platform to present and refine this work.

Funding

This research received no external funding.

Conflict of Interest statement

The author declares no conflict of interest related to this study.

Author Contributions

The author was solely responsible for study conception and design, data collection and analysis, and manuscript preparation. All work presented is original, and the author accepts full responsibility for the integrity of the content.

Competing Interests

The author declares no competing interests.

Dual Publication

This manuscript has not been previously published and is not under consideration elsewhere.

Authorship

The corresponding author confirms that they have read and agree to the journal's authorship policies and is submitting this manuscript in accordance with those requirements.

Permission to Use Third-Party Material

All figures, tables, and data presented in this manuscript were created by the author. No third-party material requiring copyright permission has been used.

Data Availability

The datasets generated and analysed during this study are available from the corresponding author upon reasonable request.

Consent to Participate

The research was formally approved by the School of Geography, Archaeology and Environmental Studies, University of the Witwatersrand, as part of my MSc minor dissertation. The study relied exclusively on publicly available satellite datasets (Landsat 8) and did not involve human participants, interviews, or personal data; no additional ethics approval or consent to participate was required.

Consent to Publish

Not applicable..

REFERENCES

1. Acosta-Caipa, K., Espinoza-Molina, J., Chambe-Vega, E., Huayna, G., & Pino-Vargas, E. (2025). Multi-level climate governance for urban heat island mitigation in Tacna, Atacama Desert, Southern Peru: An integrated approach based on the SDGs. *Inżynieria Mineralna*, *2025*(2), Article 122. https://doi.org/10.29227/im-2025-02-02-122
2. Alblooshi, H., Rezgui, Y., Beach, T., & Mustafa, M. (2026). A critical review of infrastructure resilience in fast-growing, hot, and arid cities of the Global South. *Sustainable Cities and Society, 139, Article* 107238. https://doi.org/10.1016/j.scs.2025.107238
3. Amani, M., Ghorbanian, A., Ahmadi, S. A., Kakooei, M., Moghimi, A., Mirmazloumi, S. M., Moghaddam, S. H. A., Mahdavi, S., Ghahremanloo, M., Parsian, S., Wu, Q., & Brisco, B. (2020). Google Earth Engine Cloud Computing Platform for Remote Sensing Big Data Applications: A Comprehensive Review. *IEEE Journal of Selected Topics in Applied Earth Observations and Remote Sensing*, *13*, 5326–5350. https://doi.org/10.1109/JSTARS.2020.3021052
4. Aslan, N., & Koc-San, D. (2016). Analysis of relationship between urban heat island effect and Land use/cover type using Landsat 7 ETM+ and Landsat 8 OLI images. *International Archives of the Photogrammetry, Remote Sensing and Spatial Information Sciences - ISPRS Archives*, *41*, 821–828. https://doi.org/10.5194/isprsarchives-XLI-B8-821-2016
5. Bandara, R. M. R. K., De Silva, M. R. R., Gunapravin, T., & Dissanayake, D. M. D. O. K. (2025). Assessing & mitigating urban heat island in Colombo to achieve SDG 11 and SDG 13. *International Symposium on Earth Resources Management and Environment (ISERME 2025),* 14. https://doi.org/10.31705/iserme.2025.14
6. Barrao, S., Serrano-Notivoli, R., Cuadrat, J. M., Tejedor, E., & Saz Sánchez, M. A. (2022). Characterization of the UHI in Zaragoza (Spain) using a quality-controlled hourly sensor-based urban climate network. *Urban Climate*, *44*. https://doi.org/10.1016/j.uclim.2022.101207
7. Betts, R. A., Alfieri, L., Bradshaw, C., Caesar, J., Feyen, L., Friedlingstein, P., Gohar, L., Koutroulis, A., Lewis, K., Morfopoulos, C., Papadimitriou, L., Richardson, K. J., Tsanis, I., & Wyser, K. (2018). Changes in climate extremes, freshwater availability and vulnerability to food insecurity projected at 1.5°C and 2°C global warming with a higher-resolution global climate model. *Philosophical Transactions of the Royal Society A: Mathematical, Physical and Engineering Sciences*, *376*(2119). https://doi.org/10.1098/rsta.2016.0452

8. Brom, P. (2023). A decision support tool for green infrastructure planning in the face of rapid urbanization. *Land*, *12*(2), Article 415. https://doi.org/10.3390/land12020415
9. Byakatonda, J., Parida, B. P., Moalafhi, D. B., Kenabatho, P. K., & Lesolle, D. (2020). Investigating the relationship between drought severity in Botswana and ENSO. *Natural Hazards*, *100*(1), 255–278. https://doi.org/10.1007/s11069-019-03810-1
10. Botswana Climate (2011). Temperature records of the last 47 years. https://www.worlddata.info/africa/botswana/climate.php
11. Chiguvi, D. (2022). Analysis of the Causes of Urban Sprawl and Dwelling Transformation in Urban Cities in Botswana.' *Journal of Legal, Ethical and Regulatory Issues 25,* (1). https://heinonline.org/HOL/License
12. Chiguvi, D., & Kgathi-Thite, D. (2022). Analysis of the Positive and Negative Effects of Urban Sprawl and Dwelling Transformation in Urban Cities: Case Study of Tati Siding Village in Botswana. *Journal. Legal of Ethical & Regulatory. Issues, 25, 1. https://heinonline.org/HOL/License*.
13. Chowdam, V. S., M, V. N., Kumar, G. G., & Potladurty, S. B. (2026). Remote sensing and machine learning approaches for heat island mapping and analysis: A review and framework for sustainable smart cities. *Environment, Development and Sustainability*, 1–34. https://doi.org/10.1007/s10668-025-05891-x
14. Chun, B., & Guldmann, J. M. (2018). Impact of greening on the urban heat island: Seasonal variations and mitigation strategies. Computers, Environment and Urban Systems, 71, 165–176. https://doi.org/10.1016/j.compenvurbsys.2018.05.006.
15. Cristóbal, J., Jiménez-Muñoz, J. C., Prakash, A., Mattar, C., Skoković, D., & Sobrino, J. A. (2018). An improved single-channel method to retrieve land surface temperature from the landsat-8 thermal band. Remote Sensing, 10(3). https://doi.org/10.3390/rs10030431
16. Das, D. K. (2025). Resilient and sustainable urban infrastructure in the Global South: Strategies to address climate change-linked vulnerabilities. *Urban Planning*, *10*, Article 10037. https://doi.org/10.17645/up.10037
17. Debbage, N., & Shepherd, J. M. (2015). The urban heat island effect and city contiguity. *Computers, Environment and Urban Systems*, *54*, 181–194. https://doi.org/10.1016/j.compenvurbsys.2015.08.002
18. Dutta, D., Rahman, A., Paul, S. K., & Kundu, A. (2021). Impervious surface growth and its inter-relationship with vegetation cover and land surface temperature in peri-urban areas of Delhi. *Urban Climate*, *37*. https://doi.org/10.1016/j.uclim.2021.100799

19. Engelbrecht, F. A., Steinkopf, J., Padavatan, J., & Midgley, G. F. (2024). Projections of future climate change in Southern Africa and the potential for regional tipping points. In *Sustainability of southern African ecosystems under global change: Science for management and policy interventions* (pp. 169–190). Springer International Publishing. https://doi.org/10.1007/978-3-031-57415-3_7
20. England, M. I., Dougill, A. J., Stringer, L. C., Vincent, K. E., Pardoe, J., Kalaba, F. K., & Afionis, S. (2018). Climate change adaptation and cross-sectoral policy coherence in southern Africa. *Regional Environmental Change*, *18*(7), 2059–2071. https://doi.org/10.1007/s10113-018-1283-0
21. Fashae, O., Adagbasa, E., Olusola, A., & Obateru, R. O. (2020). Land use/land cover change and land surface temperature of Ibadan and environs, Nigeria. *Environmental Monitoring and Assessment*, *192*(2), Article 109. https://doi.org/10.1007/s10661-019-8054-3
22. Feng, L., Zhao, M., Zhou, Y., Zhu, L., & Tian, H. (2020). The seasonal and annual impacts of landscape patterns on the urban thermal comfort using Landsat. *Ecological Indicators*, *110*. https://doi.org/10.1016/j.ecolind.2019.105798
23. Gökçekuş, H., Kassem, Y., & Mphinyane, L. P. (2021). Analysis of spatio-temporal rainfall trends and rainfall variability in Botswana between 1958 and 2019. *International Advanced Researches and Engineering Journal*. https://doi.org/10.35860/iarej.906557
24. Goldblatt, R., Addas, A., Crull, D., Maghrabi, A., Levin, G. G., & Rubinyi, S. (2021). Remotely sensed derived land surface temperature (LST) as a proxy for air temperature and thermal comfort at a small geographical scale. *Land*, *10*(4). https://doi.org/10.3390/land10040410
25. Gondo, R., & Mutanga, C. N. (2024). Impact of anthropological activities on land-use and land-cover changes in the lower Okavango Delta, Botswana. *Transactions of the Royal Society of South Africa*, *79*(1), 1–18. https://doi.org/10.1080/0035919X.2023.2294270
26. Hashim, B. M., Al Maliki, A., Sultan, M. A., Shahid, S., & Yaseen, Z. M. (2022). Effect of land use land cover changes on land surface temperature during 1984–2020: a case study of Baghdad city using Landsat image. *Natural Hazards*, *112*(2), 1223–1246. https://doi.org/10.1007/s11069-022-05224-y
27. Huang, X., Liu, W., Han, Y., Wang, C., Wang, H., & Hu, S. (2019). Performance evaluation and comparison of modified spectral mixture analysis method for different images of Landsat series satellites. *Sustainability (Switzerland)*, *11*(22). https://doi.org/10.3390/su11226227

28. Ibrahim, S. H., Ibrahim, N. I. A., Wahid, J., Goh, N. A., Koesmeri, D. R. A., & Nawi, M. N. M. (2018). The impact of road pavement on urban heat island (UHI) phenomenon. *International Journal of Technology*, *9*(8), 1597–1608. https://doi.org/10.14716/ijtech.v9i8.2755
29. Jimenez-Munoz, J. C., Sobrino, J. A., Skoković, D., Mattar, C., & Cristobal, J. (2014). Land surface temperature retrieval methods from Landsat-8 thermal infrared sensor data. *IEEE Geoscience and Remote Sensing Letters*, *11*(10), 1840–1843. https://doi.org/10.1109/LGRS.2014.2312032
30. Jonsson, P. (2004). Vegetation as an urban climate control in the subtropical city of Gaborone, Botswana. *International Journal of Climatology*, *24*(10), 1307–1322. https://doi.org/10.1002/joc.1064
31. Kabano, P., Lindley, S., & Harris, A. (2021). Evidence of urban heat island impacts on the vegetation growing season length in a tropical city. *Landscape and Urban Planning*, *206*. https://doi.org/10.1016/j.landurbplan.2020.103989
32. Khallef, B., Biskri, Y., Mouchara, N., & Brahamia, K. (2020). Analysis of Urban Heat Islands Using Landsat 8 OLI / TIR Data: Case of the City of Guelma (Algeria). *Asian Journal of Environment & Ecology*, 42–51. https://doi.org/10.9734/ajee/2020/v12i430167
33. Leal Filho, W., Echevarria Icaza, L., Neht, A., Klavins, M., & Morgan, E. A. (2018). Coping with the impacts of urban heat islands. A literature-based study on understanding urban heat vulnerability and the need for resilience in cities in a global climate change context. *Journal of Cleaner Production*, *171*, 1140–1149. https://doi.org/10.1016/j.jclepro.2017.10.086
34. Li, D., Bou-Zeid, E., & Oppenheimer, M. (2014). The effectiveness of cool and green roofs as urban heat island mitigation strategies. Environmental Research Letters, 9(5). https://doi.org/10.1088/1748-9326/9/5/055002
35. Liu, H., Li, J., Du, J., Zhao, B., Hu, Y., Li, D., & Yu, W. (2022). Identification of Smoke from Straw Burning in Remote Sensing Images with the Improved YOLOv5s Algorithm. *Atmosphere*, *13*(6). https://doi.org/10.3390/atmos13060925
36. Labib, M., Wibowo, A., & Shidiq, I. (2022). LST-based threshold method for detecting UHI in a complex urban landscape. *IOP Conference Series: Earth and Environmental Science*, *986*(1), 012072. https://doi.org/10.1088/1755-1315/986/1/012072
37. Lotfabadi, P., & Hançer, P. (2019). A comparative study of traditional and contemporary building envelope construction techniques in terms of thermal comfort and energy efficiency in hot and humid climates. *Sustainability (Switzerland)*, *11*(13). https://doi.org/10.3390/su11133582

38. MacLachlan, A., Biggs, E. M., Roberts, G., & Boruff, B. (2021). Sustainable city planning: A data-driven approach for mitigating urban heat. *Frontiers in Built Environment*, *6*, Article 519599. https://doi.org/10.3389/fbuil.2020.519599
39. Makvandi, M., Li, Y., Huang, J., Zhao, Y., Zhang, X., & Zhou, X. (2024). Advancing urban resilience amid rapid urbanization: An integrated interdisciplinary approach for tomorrow's climate-adaptive smart cities—A case study of Wuhan, China. *Smart Cities*, *7*(4), Article 84. https://doi.org/10.3390/smartcities7040084
40. Matenge, R. G., Parida, B. P., Letshwenyo, M. W., & Ditalelo, G. (2023). Impact of Climate Variability on Rainfall Characteristics in the Semi-Arid Shashe Catchment (Botswana) from 1981–2050. *Earth (Switzerland)*, *4*(2), 398–441. https://doi.org/10.3390/earth4020022
41. Miao, C., Li, P., Huang, Y., Sun, Y., Chen, W., & Yu, S. (2023). Coupling outdoor air quality with thermal comfort in the presence of street trees: a pilot investigation in Shenyang, Northeast China. *Journal of Forestry Research*, *34*(3), 831–839. https://doi.org/10.1007/s11676-022-01497-y
42. Mijani, N., Alavipanah, S. K., Firozjaei, M. K., Arsanjani, J. J., Hamzeh, S., & Weng, Q. (2020). Modeling outdoor thermal comfort using satellite imagery: A principal component analysis-based approach. *Ecological Indicators*, *117*. https://doi.org/10.1016/j.ecolind.2020.106555
43. Mohammad Harmay, N. S., & Choi, M. (2022). Effects of heat waves on urban warming across different urban morphologies and climate zones. *Building and Environment*, *209*. https://doi.org/10.1016/j.buildenv.2021.108677
44. Morabito, M., Crisci, A., Messeri, A., Orlandini, S., Raschi, A., Maracchi, G., & Munafò, M. (2016). The impact of built-up surfaces on land surface temperatures in Italian urban areas. *Science of the Total Environment*, *551–552*, 317–326. https://doi.org/10.1016/j.scitotenv.2016.02.029
45. Moses, O. (2017). Special Issue on Environment, Tourism and Contemporary Socio-economic Issues in the Okavango Delta and other. *Ecosystems*, *49*, 13–25. https://doi.org/10.2307/90024331
46. Mutani, G., Todeschi, V., & Beltramo, S. (2024). Synergising machine learning and remote sensing for urban heat island dynamics: A comprehensive modelling approach. *Atmosphere*, *15*(12), Article 1435. https://doi.org/10.3390/atmos15121435
47. New, M., & Bosworth, B. (2018). *What global warming of 1.5°C and higher means for Botswana and Namibia*. Climate and Development Knowledge Network. https://cdkn.org/resource/report-what-global-warming-of-1-5c-and-higher-means-for-botswana-and-namibia

48. Niang, I., Ruppel, O. C., Abdrabo, M. A., Essel, A., Lennard, C., Padgham, J., & Urquhart, P. (2014). Africa. In V. R. Barros, C. B. Field, D. J. Dokken, M. D. Mastrandrea, K. J. Mach, T. E. Bilir, M. Chatterjee, K. L. Ebi, Y. O. Estrada, R. C. Genova, B. Girma, E. S. Kissel, A. N. Levy, S. MacCracken, P. R. Mastrandrea, & L. L. White (Eds.), *Climate change 2014: Impacts, adaptation, and vulnerability. Part B: Regional aspects. Contribution of Working Group II to the Fifth Assessment Report of the Intergovernmental Panel on Climate Change* (pp. 1199–1265). Cambridge University Press. https://doi.org/10.1017/CBO9781107415386.002
49. Nkemelang, T., New, M., & Zaroug, M. (2018). Temperature and precipitation extremes under current, 1.5 °c and 2.0 °c global warming above pre-industrial levels over Botswana, and implications for climate change vulnerability. *Environmental Research Letters*, *13*(6). https://doi.org/10.1088/1748-9326/aac2f8
50. Nwogu, N., Victoria, M. F., Salman, H., & Oyetunji, A. K. (2025). Integrating GIS into flood risk management: A Global South perspective on resilience, planning, and policy. *Water*, *17*(21), Article 3149. https://doi.org/10.3390/w17213149
51. Omodasola, B. H. (2025). GeoAI for monitoring and predicting urban climate shocks: A systematic review and framework for African resilient cities. *Mikailalsys Journal of Advanced Engineering International*, *2*(3), 7558. https://doi.org/10.58578/mjaei.v2i3.7558
52. Onačillová, K., Gallay, M., Paluba, D., Péliová, A., Tokarčík, O., & Laubertová, D. (2022). Combining Landsat 8 and Sentinel-2 Data in Google Earth Engine to Derive Higher Resolution Land Surface Temperature Maps in Urban Environment. *Remote Sensing*, *14*(16). https://doi.org/10.3390/rs14164076
53. Ouma, Y. O., Tjitemisa, T., Segobye, M., Moreri, K., Nkwae, B., Maphale, L., & Manisa, B. (2021). *Urban land surface temperature variations with LULC, NDVI and NDBI in semi-arid urban environments: case study of Gaborone City, Botswana (1989–2019)*. 6. https://doi.org/10.1117/12.2595031
54. Pan, X., Mavrokapnidis, D., Ly, H.T., Moham, N. (2024). *Assessing and forecasting collective urban heat exposure with smart city digital twins*. Scientific Reports.
55. Peng, S., Piao, S., Ciais, P., Friedlingstein, P., Ottle, C., Bréon, F. M., Nan, H., Zhou, L., & Myneni, R. B. (2012). Surface urban heat island across 419 global big cities. *Environmental Science and Technology*, *46*(2), 696–703. https://doi.org/10.1021/es2030438

56. *Population and Housing Census (2022). Population of Cities, Towns, and villages*. www.statsbots.org.bw
57. Prasad, H. P. S., & Satyanarayana, A. N. V. (2023). Assessment of Outdoor Thermal Comfort Using Landsat 8 Imageries with Machine Learning Tools over a Metropolitan City of India. *Pure and Applied Geophysics*, *180*(10), 3621–3637. https://doi.org/10.1007/s00024-023-03328-5
58. Ranagalage, M., Estoque, R. C., Zhang, X., & Murayama, Y. (2018). Spatial changes of urban heat island formation in the Colombo District, Sri Lanka: Implications for sustainability planning. *Sustainability (Switzerland)*, *10*(5). https://doi.org/10.3390/su10051367
59. Rao, P., Singh, A., & Pandey, K. (2021). Time-series analysis of open data for studying urban heat island phenomenon: a geospatial approach. *Spatial Information Research*, *29*(6), 1–12. https://doi.org/10.1007/S41324-021-00401-W
60. Richard, Y., Pohl, B., Rega, M., Pergaud, J., Thevenin, T., Emery, J., Dudek, J., Vairet, T., Zito, S., & Chateau-Smith, C. (2021). Is Urban Heat Island intensity higher during hot spells and heat waves (Dijon, France, 2014–2019)? *Urban Climate*, *35*. https://doi.org/10.1016/j.uclim.2020.100747
61. Richiardi, C., Caroscio, L., Crescini, E., De Marchi, M., De Pieri, G. M., Ceresi, C., ... & Pappalardo, S. E. (2025). A global downstream approach to mapping surface urban heat islands using open data and collaborative technology. *Sustainable Geosciences: People, Planet and Prosperity*, 100006. https://doi.org/10.1016/j.susgeo.2025.100006
62. Sewwandi, & Panagopoulos. (2025). Planning Sustainable Green Blue Infrastructure in Colombo to Optimize Park Cool Island Intensity. Land. https://doi.org/10.3390/land14112164
63. Sobrino, J. A., Jiménez-Muñoz, J. C., & Paolini, L. (2004). Land surface temperature retrieval from LANDSAT TM 5. *Remote Sensing of Environment*, *90*(4), 434–440. https://doi.org/10.1016/j.rse.2004.02.003
64. Sharma, R., Pradhan, L., Kumari, M., & Bhattacharya, P. (2021). Assessing urban heat islands and thermal comfort in Noida City using geospatial technology. *Urban Climate*, *35*. https://doi.org/10.1016/j.uclim.2020.100751
65. Sufrianto, W., & Candra, O. (2022). The Effect Of Electrical Installation Trainer Media On Undergraduate Students Learning Outcomes Of Domestic Electrical Installation Practice Course. *JTEV (Jurnal Teknik Elektro Dan Vokasional)*, *8*(1), 128. https://doi.org/10.24036/jtev.v8i1.116682

66. Taha, H. (1997). Urban climates and heat islands: Albedo, evapotranspiration, and anthropogenic heat. *Energy and Buildings*, *25*(2), 99–103. [1] https://doi.org/10.1016/S0378-7788(96)00999-1
67. Tsidu, G. M. (2023). *Spatio-temporal variability of rainfall and temperature extremes over Southern Africa*. https://doi.org/10.5194/egusphere-egu23-3037
68. Ullah, N., Siddique, M. A., Ding, M., Grigoryan, S., Khan, I. A., Kang, Z., Tsou, S., Zhang, T., Hu, Y., & Zhang, Y. (2023). The Impact of Urbanization on Urban Heat Island: Predictive Approach Using Google Earth Engine and CA-Markov Modelling (2005–2050) of Tianjin City, China. *International Journal of Environmental Research and Public Health*, *20*(3). https://doi.org/10.3390/ijerph20032642
69. Ullah, N., Siddique, M. A., Ding, M., Grigoryan, S., Zhang, T., & Hu, Y. (2022). Spatiotemporal Impact of Urbanization on Urban Heat Island and Urban Thermal Field Variance Index of Tianjin City, China. *Buildings*, *12*(4). https://doi.org/10.3390/buildings12040399
70. van der Linden, N., Longden, T., Richards, J. R., Khursheed, M., Goddijn, W. M. T., van Veelen, M. J., Khan, U. R., & Christien van der Linden, M. (2019). The use of an 'acclimatisation' heatwave measure to compare temperature-related demand for emergency services in Australia, Botswana, Netherlands, Pakistan, and USA. *PLoS ONE*, *14*(3). https://doi.org/10.1371/journal.pone.0214242
71. Victoria, M. F., et al. (2025). Integrating GIS into flood risk management: A Global South perspective on resilience, planning, and policy. Water, 17(21), Article 3149. https://doi.org/10.3390/w17213149
72. Wang, F., Qin, Z., Song, C., Tu, L., Karnieli, A., & Zhao, S. (2015). An improved mono-window algorithm for land surface temperature retrieval from Landsat 8 thermal infrared sensor data. *Remote Sensing*, *7*(4), 4268–4289. https://doi.org/10.3390/rs70404268
73. Wang, L. (2025). Urban heat island monitoring and intelligent prediction method based on big data analysis. *Sustainable Energy Research*, *12*(1), Article 55. https://doi.org/10.1186/s40807-025-00195-5
74. Wang, M., Zhang, Z., Hu, T., & Liu, X. (2019). A Practical Single-Channel Algorithm for Land Surface Temperature Retrieval: Application to Landsat Series Data. Journal of Geophysical Research: Atmospheres, 124(1), 299–316. https://doi.org/10.1029/2018JD029330
75. Wijesundara, A. A. S. G., Sewwandi, B. G. N., & Panagopoulos, T. (2025). Planning sustainable green blue infrastructure in Colombo to optimize park cool island intensity. *Land*, *14*(11), Article 2164. https://doi.org/10.3390/land14112164

76. Wieszczeczynska, K. A., Tollin, N., & Spaliviero, M. (2024). Capacity building within urban climate resilience in the Global South–a literature review. *Frontiers in Sustainable Cities*, *6*, Article 1380936. https://doi.org/10.3389/frsc.2024.1380936
77. Wu, C.-F., Chen, C.-W., Lin, Y.-P., & Crossman, N. D. (2021). Climate justice planning in Global South: Applying a coupled nature–human flood risk assessment framework in a case for Ho Chi Minh City, Vietnam. *Water*, *13*(15), Article 2021. https://doi.org/10.3390/w13152021
78. Yang, C., He, X., Yan, F., Yu, L., Bu, K., Yang, J., Chang, L., & Zhang, S. (2017). Mapping the influence of land use/land cover changes on the urban heat island effect-A case study of Changchun, China. *Sustainability (Switzerland)*, *9*(2). https://doi.org/10.3390/su9020312
79. Yang, Y., Song, F., Ma, J., Wei, Z., Song, L., & Cao, W. (2022). Spatial and temporal variation of heat islands in the main urban area of Zhengzhou under the two-way influence of urbanization and urban forestry. *PLoS ONE*, *17*(8 August). https://doi.org/10.1371/journal.pone.0272626
80. Yuan, J., Antoszewski, P., Choryński, A., Gao, Y., Chai, J., & Kong, X. (2026). Urban heat island mitigation strategies: A comprehensive review of recent advances. *City and Environment Interactions*, Article 100351. https://doi.org/10.1016/j.cacint.2026.100351
81. Zhao, Q., Yu, L., Li, X., Peng, D., Zhang, Y., & Gong, P. (2021). Progress and trends in the application of google earth and google earth engine. In *Remote Sensing* (Vol. 13, Issue 18). MDPI. https://doi.org/10.3390/rs13183778
82. Zhao, Z., Ye, R., Wang, Y., & Tao, Y. (2023). How Plot Spatial Morphology Drives Surface Thermal Environment: A Spatial and Temporal Analysis of Nanjing Main City. Sustainability (Switzerland), 15(1). https://doi.org/10.3390/su15010383